Syntheses, Reactivity, and X-ray Structure Analyses of the Dimeric Pentaphosphides $[(t\mathrm{Bu}_3\mathrm{Si})_3\mathrm{P}_5\mathrm{M}_2]_2$ (M = Na, Ag) and the Bicyclo[2.1.0]pentaphosphane $(t\mathrm{Bu}_3\mathrm{Si})_3\mathrm{P}_5$

Hans-Wolfram Lerner,[a]* Günter Margraf,[a] Linda Kaufmann,[a] Jan W. Bats,[b] Michael Bolte,[a] and Matthias Wagner[a]

Keywords: Phosphorus / Phosphane / Supersilyl phosphides / Silanide

The sodium pentaphosphide dimer $[(t\mathrm{Bu}_3\mathrm{Si})_3\mathrm{P}_5\mathrm{Na}_2(\mathrm{THF})]_2$ has been synthesized in high yield from the reaction of four equivalents of the sodium silanide $t\mathrm{Bu}_3\mathrm{SiNa}$ with P_4. X-ray quality crystals of the sodium pentaphosphide dimer $[(t\mathrm{Bu}_3\mathrm{Si})_3\mathrm{P}_5\mathrm{Na}_2(\mathrm{THF})]_2$ (monoclinic, $P2_1/n$) were grown from benzene. The sodium pentaphosphide $(t\mathrm{Bu}_3\mathrm{Si})_3\mathrm{P}_5\mathrm{Na}_2$ can be oxidized with one equivalent of TCNE to give the bicyclo[2.1.0]pentaphosphane $(t\mathrm{Bu}_3\mathrm{Si})_3\mathrm{P}_5$; it also reacts with AgOCN to give the silver pentaphosphide $[(t\mathrm{Bu}_3\mathrm{Si})_3\mathrm{P}_5\mathrm{Ag}_2]_2$ (monoclinic, $P2_1/n$). Crystals of the pentaphosphane $(t\mathrm{Bu}_3\mathrm{Si})_3\mathrm{P}_5$ (monoclinic, $P2_1/c$) suitable for X-ray diffraction were obtained from hexane at –25 °C.

Introduction

The nucleophilic degradation of P_4 with $t\mathrm{Bu}_3\mathrm{SiM}$ (M = Li, Na, K) or $t\mathrm{Bu}_2\mathrm{PhSiNa}$ in a molar ratio of 1:2 leads to the tetraphosphenediides **1** $[(t\mathrm{Bu}_3\mathrm{Si})_2\mathrm{P}_4\mathrm{M}_2]$ (M = Li, Na, K) and $[(t\mathrm{Bu}_2\mathrm{PhSi})_2\mathrm{P}_4\mathrm{Na}_2]$, which dimerize in weakly polar solvents to form the octaphosphides **2** $[(t\mathrm{Bu}_3\mathrm{Si})_4\mathrm{P}_8\mathrm{M}_4]$ (M = Li, Na, K) and $[(t\mathrm{Bu}_2\mathrm{PhSi})_4\mathrm{P}_8\mathrm{Na}_4]$ (Scheme 1).[1–4]

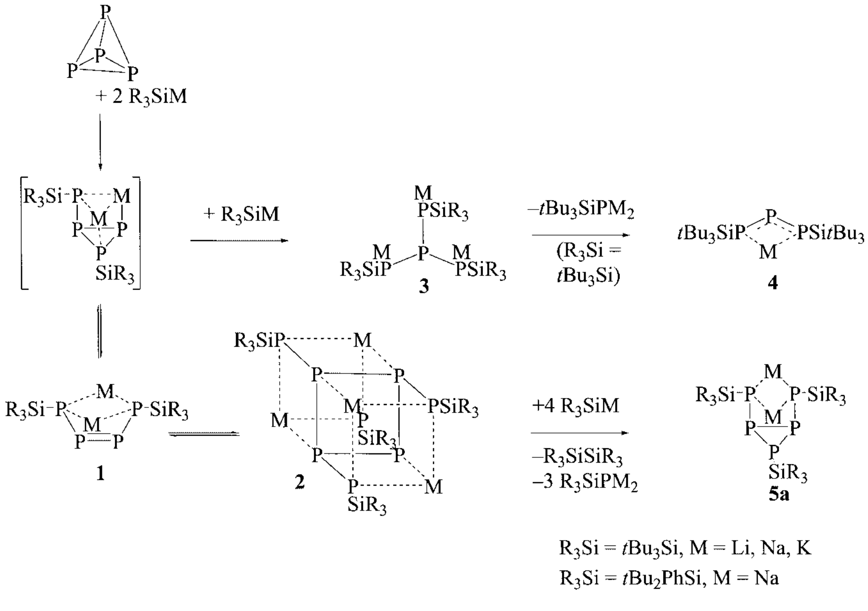

Scheme 1.

Recently we have reported the reaction of P_4 with the silanides $t\mathrm{Bu}_3\mathrm{SiM}$ (M = Li, Na) and $t\mathrm{Bu}_2\mathrm{PhSiNa}$ in a 1:3 stoichiometry, which leads cleanly to the tetraphosphides **3** $[(t\mathrm{Bu}_3\mathrm{Si})_3\mathrm{P}_4\mathrm{M}_3]$ (M = Li, Na) and $[(t\mathrm{Bu}_2\mathrm{PhSi})_3\mathrm{P}_4\mathrm{Na}_3]$, respectively.[5] In contrast, when P_4 was treated with three equivalents of $t\mathrm{Bu}_3\mathrm{SiK}$ in tetrahydrofuran, the potassium

---

[a] Institut für Anorganische Chemie, Johann Wolfgang Goethe-Universität Frankfurt am Main,
Marie-Curie-Straße 11, 60439 Frankfurt am Main, Germany
Fax: +49-69-79829260
E-mail: lerner@chemie.uni-frankfurt.de
[b] Institut für Organische Chemie, Johann Wolfgang Goethe-Universität Frankfurt am Main,
Marie-Curie-Straße 11, 60439 Frankfurt am Main, Germany

DOI: 10.1002/ejic.200400970

tetraphosphenediide [$(t\mathrm{Bu}_3\mathrm{Si})_2\mathrm{P}_4\mathrm{K}_2$] and the octaphosphide [$(t\mathrm{Bu}_3\mathrm{Si})_4\mathrm{P}_8\mathrm{K}_4$] were formed as the main products rather than the tetraphosphide [$(t\mathrm{Bu}_3\mathrm{Si})_3\mathrm{P}_4\mathrm{K}_3$].[4]

Surprisingly, treatment with tri-*tert*-butylsilylpotassium (supersilylpotassium, $t\mathrm{Bu}_3\mathrm{SiK}$) slowly transforms the supersilylated potassium tetraphosphenediide [$(t\mathrm{Bu}_3\mathrm{Si})_2\mathrm{P}_4\mathrm{K}_2$] (**$1\mathrm{K}_2$**) and the octaphosphide [$(t\mathrm{Bu}_3\mathrm{Si})_4\mathrm{P}_8\mathrm{K}_4$] (**$2\mathrm{K}_4$**) into the triphosphide [$(t\mathrm{Bu}_3\mathrm{Si})_2\mathrm{P}_3\mathrm{K}$] (**4K**) and the pentaphosphide [$(t\mathrm{Bu}_3\mathrm{Si})_3\mathrm{P}_5\mathrm{K}_2$] (**$5\mathrm{aK}_2$**), respectively.[4]

The sodium pentaphosphide [$(t\mathrm{Bu}_3\mathrm{Si})_3\mathrm{P}_5\mathrm{Na}_2(\mathrm{THF})_4$][6] is the first and only structurally characterized derivative of the pentaphosphane **5a** and is a constitutional isomer of the well-known cyclopentaphosphanes of type **5b** (Scheme 2).[7,8] Derivatives of **7a** have been described in a number of recent studies.[9–12] The cation $\mathrm{Br}_2\mathrm{P}_5^+$ features the structural motif of **7b**.[13,14] The theoretical studies of Böcker and Häser have shown that the bicyclo[2.1.0]pentaphosphane **6** (non-Baudler structure) should be stable.[15]

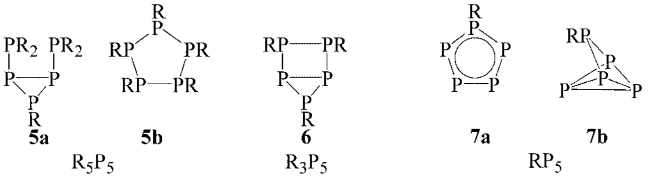

Scheme 2.

In this paper, the synthesis, reactivity and molecular structure of the bicyclo[2.1.0]pentaphosphane $(t\mathrm{Bu}_3\mathrm{Si})_3\mathrm{P}_5$, the first isolated derivative of the pentaphosphane **6**, is described. We also report here the crystal structures of the dimeric pentaphosphides [$(t\mathrm{Bu}_3\mathrm{Si})_3\mathrm{P}_5\mathrm{M}_2$]$_2$ (M = Na, Ag).

Results and Discussion

Syntheses

As we noted previously, the sodium pentaphosphide **$5\mathrm{aNa}_2$** can be generated by several routes.[6] We have now developed a synthesis by which the sodium pentaphosphide dimer [$(t\mathrm{Bu}_3\mathrm{Si})_3\mathrm{P}_5\mathrm{Na}_2(\mathrm{THF})$]$_2$ can be produced in large amounts.

The dimeric sodium pentaphosphide **[$5\mathrm{aNa}_2(\mathrm{THF})$]$_2$** is accessible by treating P_4 with four equivalents of the sodium silanide $t\mathrm{Bu}_3\mathrm{SiNa}$.[16] The first product of this reaction in THF is the sodium tetraphosphenediide [$(t\mathrm{Bu}_3\mathrm{Si})_2\mathrm{P}_4\mathrm{Na}_2$] (**$1\mathrm{Na}_2$**). The ^{31}P NMR spectrum of the resulting THF solution shows signals that can be assigned unambiguously to the sodium tetraphosphenediide **$1\mathrm{Na}_2$**. After removing the THF the reaction mixture was treated with heptane and stirred for 12 h. The main product of this procedure was the sodium octaphosphide [$(t\mathrm{Bu}_3\mathrm{Si})_4\mathrm{P}_8\mathrm{Na}_4(\mathrm{THF})_4$] [**$2\mathrm{Na}_4(\mathrm{THF})_4$**], which was characterized by X-ray crystallography. Removal of the heptane and addition of benzene, followed by stirring the resulting reaction mixture for 24 h at ambient temperature, gave the sodium pentaphosphide dimer **[$5\mathrm{aNa}_2(\mathrm{THF})$]$_2$** in 77% yield. Superdisilane was produced as a side-product in this reaction, as shown in Equation (1). The dimeric pentaphosphide **[$5\mathrm{aNa}_2(\mathrm{THF})$]$_2$** is transformed into the monomeric pentaphosphide **$5\mathrm{aNa}_2$** in tetrahydrofuran.

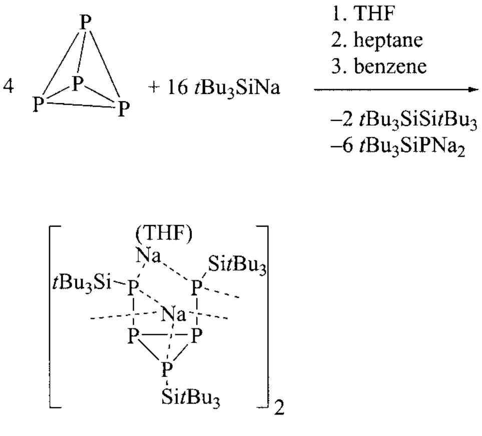

[$5\mathrm{a}(\mathrm{Na}_2)(\mathrm{THF})$]$_2$ (1)

Interestingly, the pentaphosphide **$5\mathrm{aNa}_2$** can be oxidized with TCNE to give the pentaphosphane **$6(\mathrm{Si}t\mathrm{Bu}_3)$** in quantitative yield. Treatment of this pentaphosphane with $t\mathrm{Bu}_3\mathrm{SiNa}$ leads quantitatively to the pentaphoshide **$5\mathrm{aNa}_2$** and the superdisilane $t\mathrm{Bu}_3\mathrm{SiSi}t\mathrm{Bu}_3$, as shown in Equation (2). In contrast to the reaction of **$5\mathrm{aNa}_2$** with Au$^\mathrm{I}$, where a redox process takes place,[17] the pentaphosphide **$5\mathrm{aNa}_2$** reacts with AgOCN in a metathesis reaction to give the silver pentaphosphide **[$5\mathrm{aAg}_2$]$_2$** in 53% yield [Equation (3)].

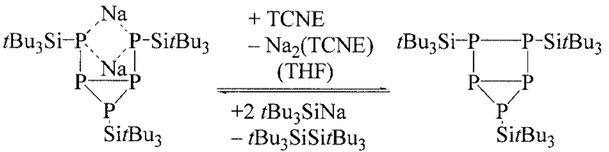

$5\mathrm{a}(\mathrm{Na}_2)$ **$6(t\mathrm{Bu}_3\mathrm{Si})$** (2)

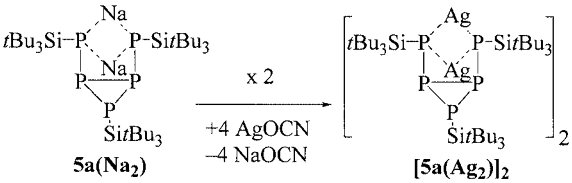

$5\mathrm{a}(\mathrm{Na}_2)$ **[$5\mathrm{a}(\mathrm{Ag}_2)$]$_2$** (3)

Surprisingly, the photolysis of **[$5\mathrm{aAg}_2$]$_2$** in a mixture of toluene and [D$_6$]benzene at ambient temperature leads to the bicyclo[1.1.0]tetraphosphane **8**[1,3] and the supersilylphosphane **9**[3] in quantitative yield [Equation (4)].

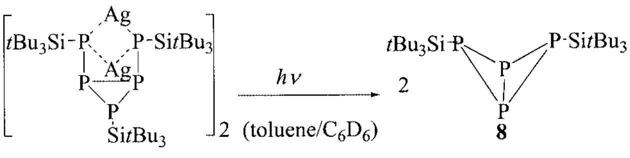

[$5\mathrm{a}(\mathrm{Ag}_2)$]$_2$ **8**

+ 2 $t\mathrm{Bu}_3\mathrm{Si}$-$\mathrm{PH}_2$
9

(4)

Reactivity of (tBu$_3$Si)$_3$P$_5$

In the thermolysis of the bicyclo[2.1.0]pentaphosphane **6(SitBu$_3$)** at 120 °C in [D$_6$]benzene the bicyclo[1.1.0]tetraphosphane **8**[1,3] and the deuterated supersilylphosphane **9(D)** were produced quantitatively, as shown in Equation (5). The formation of tBu$_3$SiPD$_2$ in the thermolysis of the bicyclo[2.1.0]pentaphosphane **6(SitBu$_3$)** can be explained by the reaction of transient supersilylphosphinidene tBu$_3$SiP with [D$_6$]benzene.

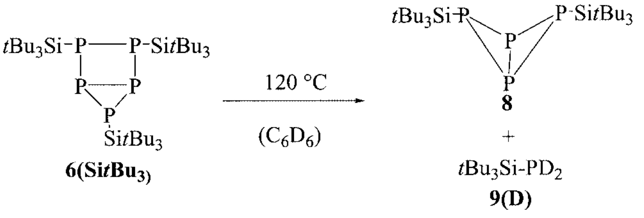

(5)

The bicyclo[2.1.0]pentaphosphane **6(SitBu$_3$)** is sensitive to oxygen and moisture. It reacts spontaneously with CF$_3$CO$_2$H to give the supersilylphosphenium trifluoroacetate [tBu$_3$SiPH$_3$][CF$_3$CO$_2$] and P$_4$. In this reaction tBu$_3$Si-O$_2$CCF$_3$ is formed as a by-product [Equation (6)].

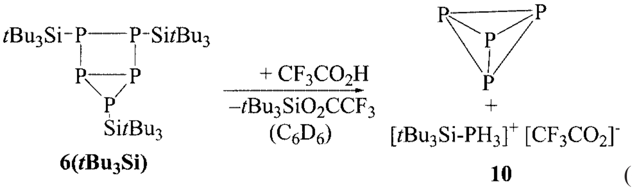

(6)

NMR Spectra

Generally, the NMR spectra of [**5aNa$_2$(THF)**]$_2$ resemble those of the monomeric sodium phosphide **5aNa$_2$**.[6] As shown in Figure 2, the signals of all P nuclei of the pentaphosphide dimer [**5aNa$_2$(THF)**]$_2$ are broadened, due to Na–P coupling. In contrast, the spectrum of monomeric pentaphosphide **5aNa$_2$** shows only broad signals for P(3) and P(4). The ^{31}P{^{1}H}NMR spectrum of **5aNa$_2$** features three multiplets with the splitting pattern of an AA′BB′MM′ spin system, as shown in Figure 2.

When [**5a(Na$_2$)(THF)**]$_2$ is dissolved in tetrahydrofuran the ^{31}P NMR spectrum becomes like that of **5aNa$_2$**. The ^{31}P{^{1}H}NMR spectrum of the silver pentaphoshide [**5aAg$_2$**]$_2$ resembles that of the dimeric sodium pentaphosphide [**5a(Na$_2$)(THF)**]$_2$. In an earlier report we discussed the NMR spectra of the monomeric pentaphosphide **5aNa$_2$** and the bicyclo[2.1.0]pentaphosphane **6(SitBu$_3$)** in detail.[6] The ^{31}P{^{1}H}NMR spectra of the sodium octaphosphide [(tBu$_3$Si)$_4$P$_8$Na$_4$(THF)$_4$] and the DME-complexed sodium octaphosphide [(tBu$_3$Si)$_4$P$_8$Na$_4$(DME)$_4$][1] exhibit the same general features (Figure 1).

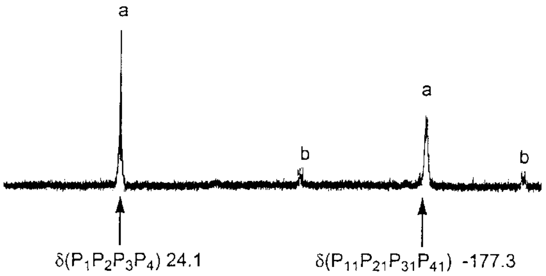

Figure 1. ^{31}P{^{1}H}NMR spectrum of the reaction solution (after stirring for 12 h in heptane) in C$_6$D$_6$ at 161.96 MHz (25 °C, external H$_3$PO$_4$). Signal of (a) sodium octaphosphide [(tBu$_3$Si)$_4$-P$_8$Na$_4$(THF)$_4$] and (b) dimeric pentaphosphide [(tBu$_3$Si)$_3$-P$_5$Na$_2$(THF)]$_2$.

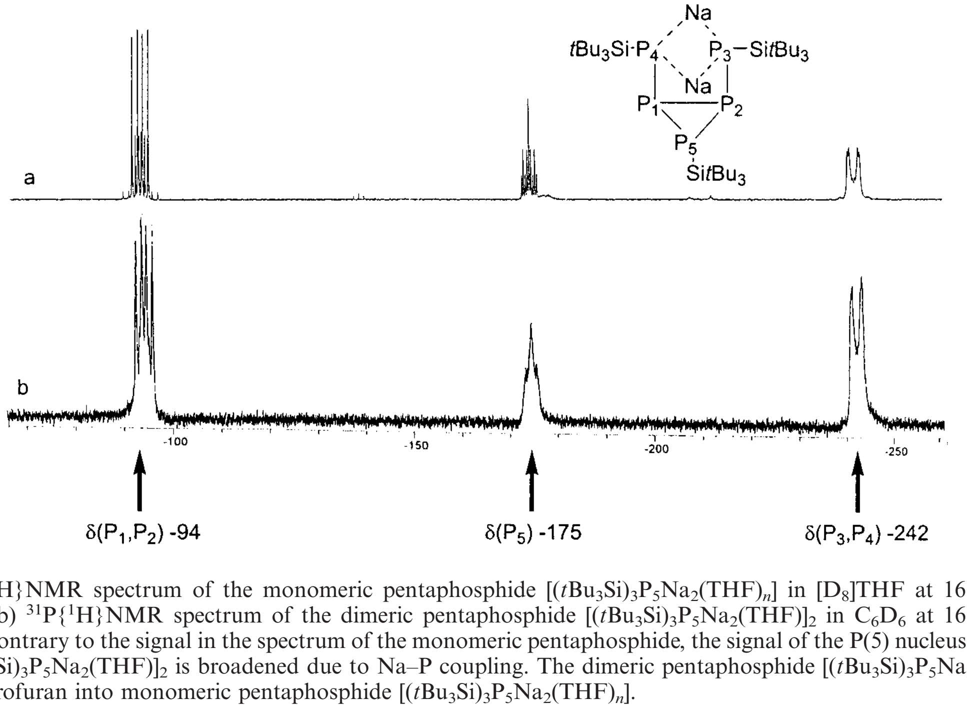

Figure 2. (a) ^{31}P{^{1}H}NMR spectrum of the monomeric pentaphosphide [(tBu$_3$Si)$_3$P$_5$Na$_2$(THF)$_n$] in [D$_8$]THF at 161.96 MHz (25 °C, external H$_3$PO$_4$). (b) ^{31}P{^{1}H}NMR spectrum of the dimeric pentaphosphide [(tBu$_3$Si)$_3$P$_5$Na$_2$(THF)]$_2$ in C$_6$D$_6$ at 161.96 MHz (25 °C; external H$_3$PO$_4$). Contrary to the signal in the spectrum of the monomeric pentaphosphide, the signal of the P(5) nucleus of the pentaphosphide dimer [(tBu$_3$Si)$_3$P$_5$Na$_2$(THF)]$_2$ is broadened due to Na–P coupling. The dimeric pentaphosphide [(tBu$_3$Si)$_3$P$_5$Na$_2$(THF)]$_2$ is transformed in tetrahydrofuran into monomeric pentaphosphide [(tBu$_3$Si)$_3$P$_5$Na$_2$(THF)$_n$].

Structure of the Sodium Octaphosphide $[(t\mathrm{Bu}_3\mathrm{Si})_4\mathrm{P}_8\mathrm{Na}_4(\mathrm{THF})_4]$

Figure 3 shows the molecular structure of the sodium octaphosphide $[(t\mathrm{Bu}_3\mathrm{Si})_4\mathrm{P}_8\mathrm{Na}_4(\mathrm{THF})_4]$ (monoclinic, $P2_1/n$); selected bond lengths and angles are listed in the corresponding figure caption. The structure of $[(t\mathrm{Bu}_3\mathrm{Si})_4\mathrm{P}_8\mathrm{Na}_4(\mathrm{THF})_4]$ shows two symmetrically independent molecules in the unit cell. The central core of $[(t\mathrm{Bu}_3\mathrm{Si})_4\mathrm{P}_8\mathrm{Na}_4(\mathrm{THF})_4]$ possesses the structure of a double cube with four P atoms in the second layer and two P and two Na atoms in the first and third layers. The corners of the first and the third layer in these cubes are alternately occupied by two P and two Na atoms [molecule A: P–Na–P 79.58(16)°, Na–P–Na 86.27(16)°; molecule B: P–Na–P 80.03(19)°, Na–P–Na 84.53(19)°]. A similar structural motif has also been found for $[(t\mathrm{Bu}_3\mathrm{Si})_4\mathrm{P}_8\mathrm{Na}_4(\mathrm{DME})_4]$.[1] Apart from the three P atoms, the Na atom in $[(t\mathrm{Bu}_3\mathrm{Si})_4\mathrm{P}_8\mathrm{Na}_4(\mathrm{THF})_4]$ is coordinated by one molecule of tetrahydrofuran. In contrast to the pentacoordinate Na atoms in $[(t\mathrm{Bu}_3\mathrm{Si})_4\mathrm{P}_8\mathrm{Na}_4(\mathrm{DME})_4]$, the sodium centers of $[(t\mathrm{Bu}_3\mathrm{Si})_4\mathrm{P}_8\mathrm{Na}_4(\mathrm{THF})_4]$ are four-coordinate. The bond lengths and angles of the THF- and DME-solvated sodium octaphosphides $[(t\mathrm{Bu}_3\mathrm{Si})_4\mathrm{P}_8\mathrm{Na}_4(\mathrm{L})_4]$ are quite similar.

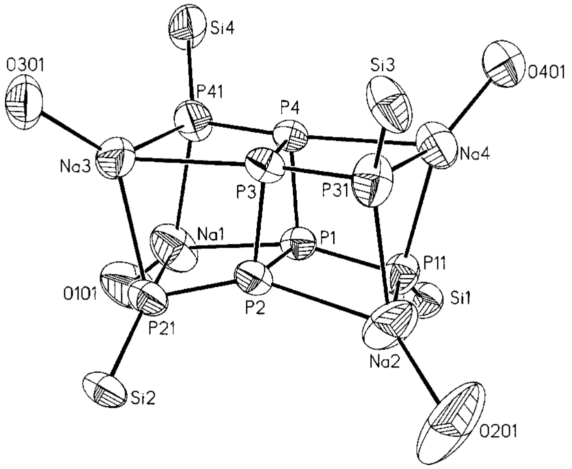

Figure 3. Thermal ellipsoid plot of $[\mathbf{2Na_4(THF_4)}]$ (molecule A), showing the atomic numbering scheme. The displacement ellipsoids are drawn at the 50% probability level. *t*Bu groups have been omitted for clarity. Selected bond lengths [Å] and angles [°]: P–Na 2.843(6) (av.), P–Si 2.210(5) (av.), Na–O 2.243(9) (av.), P(1)–P(11) 2.164(4), P(1)–P(4) 2.251(4), P(1)–P(2) 2.260(4), P(2)–P(21) 2.164(4), P(2)–P(3) 2.271(4), P(3)–P(31) 2.180(4), P(3)–P(4) 2.267(4), P(4)–P(41) 2.184(4), P(2)–P(21) 2.164(4), P(2)–P(3) 2.271(4), P(3)–P(31) 2.180(4), P(3)–P(4) 2.267(4), P(4)–P(41) 2.184(4); P(11)–P(1)–P(4) 108.68(15), P(21)–P(2)–P(3) 110.75(16), P(31)–P(3)–P(2) 95.53(15), P(11)–P(1)–P(2) 102.64(16), P(21)–P(2)–P(1) 102.17(16), P(31)–P(3)–P(4) 103.37(15), P(4)–P(1)–P(2) 89.91(14), P(1)–P(2)–P(3) 89.29(14), P(4)–P(3)–P(2) 89.23(14), P(41)–P(4)–P(1) 96.63(15), P(41)–P(4)–P(3) 102.25(15), P(1)–P(4)–P(3) 89.63(13), P(11)–P(1)–P(4) 108.68(15), P(11)–P(1)–P(2) 102.64(16), P(4)–P(1)–P(2) 89.91(14), P(21)–P(2)–P(1) 102.17(16), P(21)–P(2)–P(3) 110.75(16), P(1)–P(2)–P(3) 89.29(14), P(31)–P(3)–P(4) 103.37(15), P(31)–P(3)–P(2) 95.53(15), P(4)–P(3)–P(2) 89.23(14), P(41)–P(4)–P(1) 96.63(15), P(41)–P(4)–P(3) 102.25(15), P(1)–P(4)–P(3) 89.63(13).

Structure of the Sodium Pentaphosphide Dimer $[(t\mathrm{Bu}_3\mathrm{Si})_3\mathrm{P}_5\mathrm{Na}_2(\mathrm{THF})]_2$

X-ray quality crystals of the sodium pentaphosphide dimer $[\mathbf{5aNa_2(THF)}]_2$ were grown from benzene solution at ambient temperature. It crystallizes in the monoclinic space group $P2_1/n$, and the unit cell contains two formula units. As depicted in Figure 4, the two pentaphosphide dianions $[(t\mathrm{Bu}_3\mathrm{Si})_3\mathrm{P}_5]^{2-}$ are bridged by two Na cations to form a dimer in the solid state. The sodium pentaphosphide dimer $[\mathbf{5aNa_2(THF)}]_2$ features four P–Na contacts for the two bridging Na atoms and three P–Na contacts for the terminal Na atom. Apart from these three P atoms, the two terminal Na atoms are coordinated by one molecule of tetrahydrofuran. In contrast to the trigonal-planar sodium atom Na(2), the Na(1) center is four-coordinate in $[\mathbf{5aNa_2(THF)}]_2$. The bond lengths and angles of the sodium pentaphosphide dimer $[\mathbf{5aNa_2(THF)}]_2$ are similar to those of the monomeric sodium pentaphosphide $\mathbf{5aNa_2}$ (see caption to Figure 4).

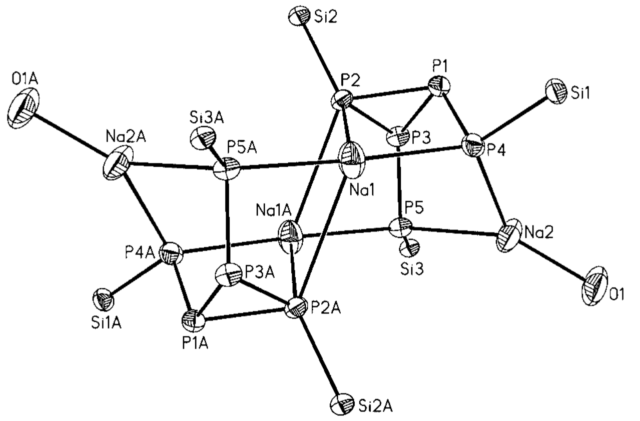

Figure 4. Thermal ellipsoid plot of $[\mathbf{5aNa_2(THF)}]_2$ showing the atom numbering scheme. The displacement ellipsoids are drawn at the 50% probability level. The *t*Bu groups of the pentaphosphide and the CH_2 units of the THF have been omitted for clarity. Selected bond lengths [Å] and angles [°]: P(1)–P(4) 2.1937(16), P(1)–P(3) 2.2393(15), P(1)–P(2) 2.2413(15), P(2)–P(3) 2.2287(15), P(2)–Si(2) 2.3150(15), P(2)–Na(1) 3.051(2), P(2)–Na(1A) 3.385(2), P(3)–P(5) 2.1866(15), P(4)–Si(1) 2.2612(15), P(4)–Na(2) 2.805(2), P(4)–Na(1) 2.846(2), P(5)–Si(3) 2.2648(15), P(5)–Na(2) 2.812(2); P(5)–Na(1A) 2.836(2), Na(1)–P(5A) 2.836(2), Na(1)–P(2A) 3.385(2), P(4)–P(1)–P(3) 111.46(6), P(4)–P(1)–P(2) 104.72(6), P(3)–P(1)–P(2) 59.66(5), P(3)–P(2)–P(1) 60.13(5). Symmetry transformations used to generate equivalent atoms: #1 $-x + 1$, $-y + 1$, $-z + 1$.

Structure of the Silver Pentaphosphide Dimer $[(t\mathrm{Bu}_3\mathrm{Si})_3\mathrm{P}_5\mathrm{Ag}_2]_2$

X-ray quality crystals of the silver pentaphosphide dimer $[\mathbf{5aAg_2}]_2$ were grown from a toluene solution at 5 °C. It crystallizes in the monoclinic space group $P2_1/n$. The unit cell contains two formula units and two molecules of toluene. As depicted in Figures 5 and 6, the two pentaphosphide dianions $[(t\mathrm{Bu}_3\mathrm{Si})_3\mathrm{P}_5]^{2-}$ cap a square-planar four-membered Ag_4 ring that contains a crystallographic inversion center at the midpoint of the molecule. The conformation of the pentaphosphide group is very similar to that of the related group in the crystal structure of **[5aNa$_2$(THF)]$_2$**. Figure 5 shows that the atoms P(1) and P(3) are coordinated to two Ag atoms, while P(2) is coordinated to only one Ag atom. The Ag–P distances range from 2.368(1) to 2.626(1) Å. The shortest Ag···Ag distances are 2.8985(5) and 3.0042(5) Å. The diagonal Ag2···Ag2′ distance of 3.3679(7) Å is slightly longer. The molecule shows nine intramolecular C–H···P contacts with H···P distances of between 2.61 and 2.88 Å. The crystal structure of **[5aAg$_2$]$_2$** features no short intermolecular contacts.

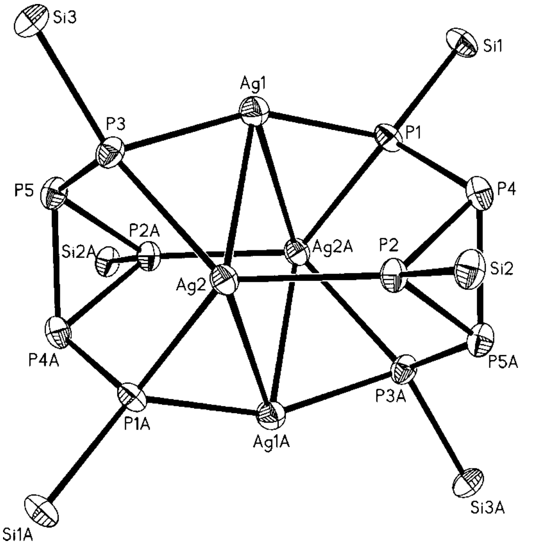

Figure 5. Thermal ellipsoid plot of **[5aAg$_2$]$_2$** showing the atom numbering scheme. The displacement ellipsoids are drawn at the 50% probability level. *t*Bu groups have been omitted for clarity. Selected bond lengths [Å] and angles [°]: Ag(1)–P(1) 2.3678(9), Ag(1)–P(3) 2.3916(9), Ag(1)–Ag(2) 2.8985(5), Ag(1)–Ag(2A) 3.0042(5), Ag(2)–P(1A) 2.5315(9), Ag(2)–P(2) 2.5436(9), Ag(2)–P(3) 2.6258(9), Ag(2)–Ag(1A) 3.0041(5), Ag(2)–Ag(2A) 3.3679(7), P(1)–P(4) 2.1820(13), P(1)–Si(1) 2.2786(12), P(1)–Ag(2A) 2.5315(9), P(3)–P(5) 2.1735(12), P(3)–Si(3) 2.2926(12), P(2)–P(4) 2.2031(12), P(2)–P(5A) 2.2371(12), P(2)–Si(2) 2.3349(12), P(4)–P(5A) 2.2528(13), Si(2)–C(17) 1.933(4), Si(2)–C(13) 1.944(4), Si(2)–C(21) 1.948(4), P(5)–P(2A) 2.2371(12), P(5)–P(4A) 2.2528(13); P(1)–Ag(1)–P(3) 154.41(3), P(1)–Ag(1)–Ag(2) 99.61(2), P(3)–Ag(1)–Ag(2) 58.59(2), P(1)–Ag(1)–Ag(2A) 54.69(2), P(3)–Ag(1)–Ag(2A) 101.94(2), Ag(2)–Ag(1)–Ag(2A) 69.555(14), P(1A)–Ag(2)–P(2) 131.19(3), P(1A)–Ag(2)–P(3) 94.89(3), P(2)–Ag(2)–P(3) 131.31(3), P(1A)–Ag(2)–Ag(1) 124.80(2), P(2)–Ag(2)–Ag(1) 85.07(2), P(3)–Ag(2)–Ag(1) 51.02(2), P(1A)–Ag(2)–Ag(1A) 49.75(2), P(2)–Ag(2)–Ag(1A) 85.80(2), P(3)–Ag(2)–Ag(1A) 125.04(2), Ag(1)–Ag(2)–Ag(1A) 110.447(14), P(1A)–Ag(2)–Ag(2A) 85.11(2), P(2)–Ag(2)–Ag(2A) 81.99(2), P(3)–Ag(2)–Ag(2A) 88.32(2), Ag(1)–Ag(2)–Ag(2A) 56.700(10), Ag(1A)–Ag(2)–Ag(2A) 53.747(10). Symmetry transformations used to generate equivalent atoms: #1 $-x + 1$, $-y$, $-z + 2$.

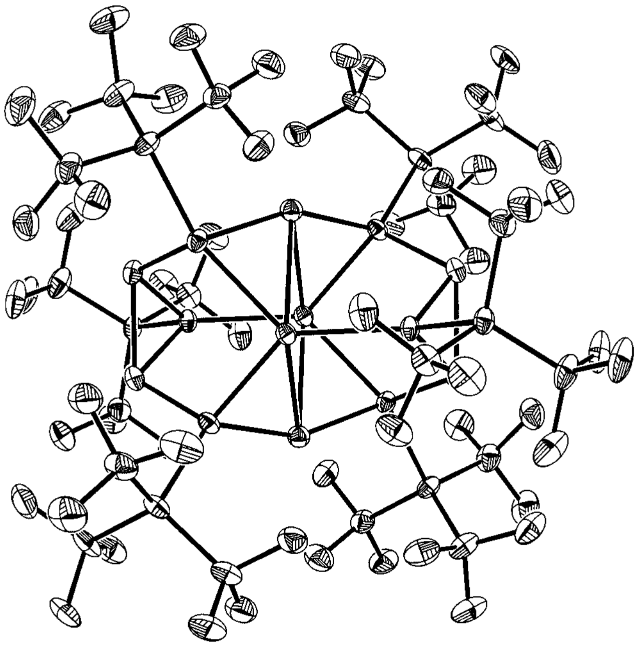

Figure 6. Thermal ellipsoid plot of **[5aAg$_2$]$_2$**. The displacement ellipsoids are drawn at the 50% probability level. The H atoms have been omitted for clarity.

Structure of the Pentaphosphane 6(Si*t*Bu$_3$)

The crystal structure of the bicyclo[2.1.0]pentaphosphane **6(Si*t*Bu$_3$)** is shown in Figures 7 and 8. X-ray quality

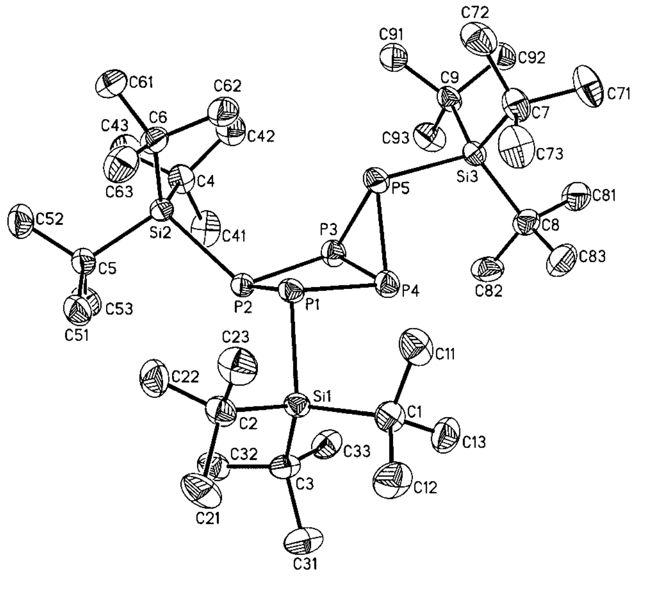

Figure 7. Thermal ellipsoid plot of **6(Si*t*Bu$_3$)** showing the atomic numbering scheme. The displacement ellipsoids are drawn at the 50% probability level. *t*Bu groups have been omitted for clarity. Selected bond lengths [Å] and angles [°]: P(1)–P(4) 2.2410(8), P(1)–P(2) 2.2537(7), P(1)–Si(1) 2.3266(7), P(2)–P(3) 2.2414(8), P(2)–Si(2) 2.3341(8), P(3)–P(5) 2.2184(8), P(3)–P(4) 2.2279(8), P(4)–P(5) 2.1862(8), P(5)–Si(3) 2.3079(8); P(4)–P(1)–P(2) 87.16(3), P(3)–P(2)–P(1) 90.34(3), P(5)–P(3)–P(4) 58.90(2), P(5)–P(3)–P(2) 105.08(3), P(4)–P(3)–P(2) 87.78(3), P(5)–P(4)–P(3) 60.33(2), P(5)–P(4)–P(1) 94.47(3), P(3)–P(4)–P(1) 91.02(3), P(4)–P(5)–P(3) 60.77(2). Symmetry transformations used to generate equivalent atoms: #1 $-x + 2$, $-y + 2$, $-z + 1$.

crystals were grown from hexane at –25 °C. It cocrystallizes with hexane in the monoclinic space group $P2_1/c$. The unit cell contains four formula units. It is interesting to note that (tBu$_3$Si)$_3$P$_5$ is the first structurally characterized pentaphosphane that features a bicyclus formed by annulated three- and four-membered rings in the solid state. The calculated strain energy of cyclotetraphosphane is lower (27 kcal mol^{-1}) than that of cyclobutane,[9] but only a limited number of compounds are known with a P$_4$-ring structure.[18–20] Generally, three- and four-membered ring systems of phosphorus are destabilized relative to five-membered ring structures.[7,15] The central core of this bicyclo[2.1.0]pentaphosphane possesses a distorted envelope structure, as shown in Figure 7. The molecular structure of **6(Si*t*Bu$_3$)** features six P–P bonds of around 2.2281(8) Å (av.). These distances are in the range of P–P single bonds. The four-membered ring in **6(Si*t*Bu$_3$)** is not planar, as confirmed by torsion angles of ±14.46(3)° (av.). The supersilyl groups at the P$_4$-ring are mutually *trans*. No significant variations between the P–Si bonds [2.3229(8) Å av.] are observed.

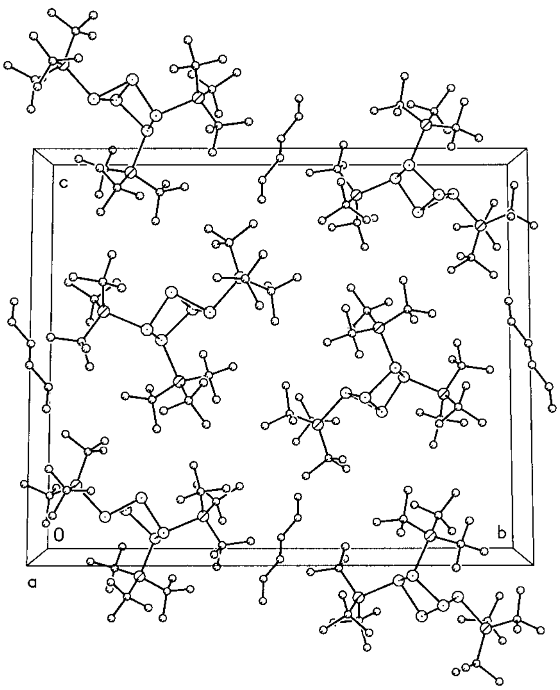

Figure 8. Crystal packing diagram of **6(Si*t*Bu$_3$)**.

Conclusions

In summary, it has been shown that the sodium pentaphosphide dimer **[5aNa$_2$(THF)]$_2$** can be cleanly prepared from tBu$_3$SiNa and white phosphorus. The sodium pentaphosphide **5aNa$_2$** can be oxidized with one equivalent of TCNE to give the bicyclo[2.1.0]pentaphosphane (tBu$_3$Si)$_3$P$_5$ [**6(Si*t*Bu$_3$)**]. On the other hand, the pentaphosphide **5aNa$_2$** reacts with AgOCN to give the silver phosphide **[5aAg$_2$]$_2$** in 53% yield.

The bicyclo[2.1.0]pentaphosphane **6(Si*t*Bu$_3$)** is sensitive to protonolysis, yielding the supersilylphosphenium cation [tBu$_3$SiPH$_3$.]$^+$. Thermolysis of this compound in C$_6$D$_6$ at 120 °C gives the 1,4-bis(supersilyl)bicyclo[1.1.0]tetraphosphane (tBu$_3$Si)$_2$P$_4$ and the deuterio supersilylphosphane tBu$_3$SiPD$_2$ quantitatively.

The sodium octaphosphide **2Na$_4$(THF$_4$)**, the pentaphosphide dimers **[5aNa$_2$(THF)]$_2$** and **[5aAg$_2$]$_2$**, and the bicyclo[2.1.0]pentaphosphane **6(Si*t*Bu$_3$)** have been studied by X-ray crystallography. The phosphane **6(Si*t*Bu$_3$)** represents a novel type of pentaphosphane featuring a bicyclus formed by annulated three- and four-membered rings in the solid state.

Experimental Section

General Remarks: All experiments were carried out under dry argon with strict exclusion of air and moisture using standard Schlenk techniques. tBu$_3$SiNa[16] was prepared according to literature procedures. All other starting materials were purchased from commercial sources and used without further purification. The solvents (benzene, toluene, tetrahydrofuran) were distilled from sodium/benzophenone prior to use. C$_6$D$_6$ was dried over molecular sieves and stored under dry nitrogen.

The NMR spectra were recorded on a Bruker AM 250, a Bruker DPX 250, or a Bruker Avance 400 spectrometer. The ^{29}Si NMR spectra were recorded using the INEPT pulse sequence with empirically optimized parameters for polarization transfer from the tBu substituents.

Synthesis of [(tBu$_3$Si)$_3$P$_5$Na$_2$(THF)]$_2$: A solution of tBu$_3$SiNa (55.2 mmol) in tetrahydrofuran (100 mL) was added to a solution of freshly sublimed P$_4$ (1.456 g, 11.74 mmol) in 50 mL of tetrahydrofuran at –78 °C and stirred for 4 h. According to the ^{31}P NMR spectrum the tetraphosphide (tBu$_3$Si)$_2$P$_4$Na$_2$ was formed as the main product. After all volatile compounds were removed in vacuo the reaction mixture was treated with 50 mL of heptane and stirred for 12 h at ambient temperature. The product of this procedure was the sodium octaphosphide [(tBu$_3$Si)$_4$P$_8$Na$_4$(THF)$_4$] (by ^{31}P NMR spectroscopy; Figure 1). Crystals of the sodium octaphosphide [(tBu$_3$Si)$_4$P$_8$Na$_4$(THF)$_4$] suitable for X-ray diffraction were obtained in an NMR tube from [D$_6$]benzene at room temperature. The ^{31}P NMR spectrum of the reaction solution after stirring in heptane for 12 h showed the signal of [(tBu$_3$Si)$_4$P$_8$Na$_4$(THF)$_4$] (main product 85% P atoms) and the dimeric sodium pentaphosphide [(tBu$_3$Si)$_3$P$_5$Na$_2$(THF)]$_2$ (minor component 15% P atoms; Figure 2). After the heptane was exchanged for benzene and the resulting reaction mixture was stirred again for 24 h at ambient temperature the sodium pentaphosphide dimer [(tBu$_3$Si)$_3$P$_5$Na$_2$(THF)]$_2$ was formed. X-ray quality crystals of [(tBu$_3$Si)$_3$P$_5$Na$_2$(THF)]$_2$ were grown after the reaction mixture had been concentrated in vacuo to a volume of 15 mL and kept at ambient temperature. Yield: 6.306 g (77%).

Selected Data for (tBu$_3$Si)$_2$P$_4$Na$_2$: ^{1}H NMR ([D$_8$]THF, internal TMS): δ = 1.10 (br., 54 H, tBu) ppm. ^{13}C{^{1}H}NMR ([D$_8$]THF, internal TMS): δ = 25.5 (br., *C*Me$_3$), 32.5 (br., C*Me$_3$*) ppm. ^{29}Si{^{1}H}NMR ([D$_8$]THF, external TMS): δ = 22.7 (m, SitBu$_3$) ppm. ^{31}P{^{1}H}NMR (25 °C; external H$_3$PO$_4$): δ = 403.0 (m, $^1J_{P2,P3}$ = –502.6, $^1J_{P1,P2}$ = $^1J_{P3,P4}$ = –432.3, $^2J_{P1,P3}$ = $^2J_{P2,P4}$ = 33.87 Hz, P$_2$, P$_3$), –5.1 (m, $^3J_{P1,P4}$ = 184.1, $^1J_{P1,P2}$ = $^1J_{P3,P4}$ = –448.83, $^2J_{P1,P3}$ = $^2J_{P2,P4}$ = –34.7 Hz, P$_1$, P$_4$) ppm.

Selected Data for $(tBu_3Si)_4P_8Na_4(THF)_4$: ^1H NMR (C_6D_6, internal TMS): δ = 1.30 (br., 108 H, *t*Bu), 1.41 (m, 16 H, CH_2), 3.59 (m, 16 H, OCH_2) ppm. $^{13}C\{^1H\}$NMR (C_6D_6, internal TMS): δ = 25.9 (br., *C*Me$_3$), 33.0 (br., C*Me$_3$*), 25.3 (s, *C*H$_2$), 68.0 (s, O*C*H$_2$) ppm. $^{29}Si\{^1H\}$NMR (C_6D_6, internal TMS): δ = 19.8 (m, Si*t*Bu$_3$) ppm. $^{31}P\{^1H\}$NMR (25 °C; external H_3PO_4): δ = 24.1 (m, P_1, P_2, P_3, P_4), –177.3 (m, P_{11}, P_{21}, P_{31}, P_{41}) ppm.

Selected Data for $[(tBu_3Si)_3P_5Na_2(THF)]_2$: ^1H NMR (C_6D_6, internal TMS): δ = 1.28 (br., 54 H, *t*Bu), 1.26 (br., 27 H, *t*Bu), 1.40 (m, 8 H, CH_2), 3.54 (m, 8 H, OCH_2) ppm. $^{13}C\{^1H\}$NMR (C_6D_6, internal TMS): δ = 25.7 (br., *C*Me$_3$), 25.9 (br., *C*Me$_3$), 32.6 (br., C*Me$_3$*), 33.0 (br., C*Me$_3$*), 25.1 (s, *C*H$_2$), 68.0 (s, O*C*H$_2$) ppm. $^{29}Si\{^1H\}$NMR (C_6D_6, external TMS): δ = 30.8 (m, 2 Si*t*Bu$_3$), 17.8 (m, Si*t*Bu$_3$) ppm. $^{31}P\{^1H\}$NMR (see Figure 2).

Synthesis of $[(tBu_3Si)_3P_5Ag_2]_2$: AgOCN (0.300 g, 2 mmol) was added to a solution of $(tBu_3Si)_3P_5Na_2$ (1 mmol) in 30 mL of tetrahydrofuran at –78 °C and stirred for 12 h. After warming to room temperature the solvent was removed in vacuo. The solid reaction product was extracted into 15 mL of toluene (brown solution). After filtration, $[(tBu_3Si)_3P_5Ag_2]_2$ was crystallized from the toluene filtrate at –25 °C. The NMR spectra of the filtrate show small signals which can be assigned to the bicyclo[2.1.0]pentaphosphane $(tBu_3Si)_3P_5$. Yield: 1.125 g (53%).

Selected Data for $[(tBu_3Si)_3P_5Ag_2]_2$: ^1H NMR (C_6D_6, internal TMS): δ = 1.38 (br., 27 H, *t*Bu), 1.51 (br., 54 H, *t*Bu) ppm. $^{13}C\{^1H\}$NMR (C_6D_6, internal TMS): δ = 25.2 (br., *C*Me$_3$), 25.4 (br., *C*Me$_3$), 32.4 (br., C*Me$_3$*), 32.6 (br., C*Me$_3$*) ppm. $^{29}Si\{^1H\}$NMR (C_6D_6, external TMS): δ = 32.2 (m, 2 Si*t*Bu$_3$), 18.9 (m, Si*t*Bu$_3$) ppm. $^{31}P\{^1H\}$NMR (25 °C, C_6D_6, external H_3PO_4): δ = –97.2 (m, P_1, P_3), –160.6 (m, P_2), –252.8 (m, P_4, P_5) ppm.

Synthesis of the Bicyclo[2.1.0]pentaphosphane $(tBu_3Si)_3P_5$: TCNE (0.855 g, 6.39 mmol) in tetrahydrofuran (20 mL) was added to a solution of $(tBu_3Si)_3P_5Na_2$ (6.28 mmol) in 30 mL tetrahydrofuran at –78 °C and stirred for 5 h. After heating to room temperature the solvent was removed in vacuo. The solid reaction product was extracted into 30 mL of hexane (yellow solution). After filtration, $(tBu_3Si)_3P_5$ was crystallized from the hexane filtrate at –25 °C. Yield: 3.217 g (62%).

Selected Data for $(tBu_3Si)_3P_5$: Thermal decomposition of $(tBu_3Si)_3P_5$: 153 °C. ^1H NMR (C_6D_6, internal TMS): δ = 1.30 (br., 54 H, *t*Bu), 1.29 (br., 27 H, *t*Bu) ppm. $^{13}C\{^1H\}$NMR (C_6D_6, internal TMS): δ = 26.0 (d, $^2J_{C,P}$ = 6.11 Hz, *C*Me$_3$), 26.5 (d, $^2J_{C,P}$ = 6.09 Hz, *C*Me$_3$), 26.7 (d, $^2J_{C,P}$ = 5.96 Hz, *C*Me$_3$), 31.9 (br., C*Me$_3$*), 31.4 (br., C*Me$_3$*), 32.8 (br., C*Me$_3$*) ppm. $^{29}Si\{^1H\}$NMR (C_6D_6, external TMS): δ = 25.8 (m, Si*t*Bu$_3$), 24.0 (m, Si*t*Bu$_3$). 23.2 (m, Si*t*Bu$_3$) ppm. $^{31}P\{^1H\}$NMR (25 °C, C_6D_6, external H_3PO_4): δ = –77.9 (m, $^1J_{P1,P5}$ = –154.1, $^1J_{P4,P5}$ = –143.4, $^2J_{P2,P5}$ = 115.5, $^2J_{P3,P5}$ = 44.0 Hz, P_5), –121.8 (m, $^1J_{P1,P3}$ = –115.3, $^1J_{P2,P3}$ = –231.6, $^1J_{P3,P4}$ = –236.7, $^2J_{P3,P5}$ = 44.0 Hz, P_3), –130.6 (m, $^1J_{P3,P4}$ = –236.7, $^1J_{P4,P5}$ = –143.4, $^2J_{P1,P4}$ = 12.0, $^2J_{P2,P4}$ = 13.4 Hz, P_4), –135.9 (m, $^1J_{P1,P2}$ = –193.3, $^1J_{P1,P3}$ = –115.3, $^1J_{P1,P5}$ = –154.1, $^2J_{P1,P4}$ = 12.0 Hz, P_1), –211.1 (m, $^1J_{P1,P2}$ = –193.3, $^1J_{P2,P3}$ = –231.6, $^2J_{P2,P4}$ = 13.4, $^2J_{P2,P5}$ = 115.5 Hz, P_2) ppm. $C_{36}H_{81}P_5Si_3$ (753.16): calcd. C 57.41, H 10.84; found C 55.08, H 9.94. MS-EI: *m*/*z* (%) = 753 (5) [M]$^+$, 554 (100) [M – Si*t*Bu$_3$]$^+$.

Table 1. Crystallographic data and further details of the structure determination of **[2Na$_4$(THF$_4$)]**, **[5aNa$_2$(THF)]$_2$**, **[5aAg$_2$]$_2$**, and **6(Si*t*Bu$_3$)**.

	[2Na$_4$(THF$_4$)]	[5aNa$_2$(THF)]$_2$	[5aAg$_2$]$_2$	6(Si*t*Bu$_3$)
Empirical formula	$C_{64}H_{140}Na_4O_4P_8Si_4$	$C_{80}H_{178}Na_4O_2P_{10}Si_6$	$C_{86}H_{178}Ag_4P_{10}Si_6$	$C_{39}H_{88}P_5Si_3$
Color	orange	orange	brown	yellow
Formula mass	1425.84	1742.42	2122.00	796.21
Crystal system	monoclinic	monoclinic	monoclinic	monoclinic
Space group	$P2_1/n$	$P2_1/n$	$P2_1/n$	$P2_1/c$
a [Å]	34.116(6)	15.8178(16)	17.834(3)	8.7088(6)
b [Å]	13.758(3)	14.5808(9)	15.224(2)	25.9478(19)
c [Å]	36.576(6)	23.062(2)	20.102(2)	21.8754(15)
α [°]	90	90	90	90
β [°]	91.276(7)	95.367(8)	97.672(11)	97.021(5)
γ [°]	90	90	90	90
V [Å^3], Z	17163(6), 8	5295.6(8), 2	5408.9(12), 2	4906.2(6), 4
$D_{calcd.}$ [Mg/m^3]	1.104	1.093	1.303	1.078
μ(Mo-K_α) [mm^{-1}]	0.277	0.284	0.965	0.284
F(000)	6208	1904	2232	1756
Crystal size [mm^3]	0.25 × 0.21 × 0.19	0.31 × 0.11 × 0.08	0.40 × 0.40 × 0.34	0.47 × 0.21 × 0.19
Diffractometer	Stoe-IPDS-II	Stoe-IPDS-II	Siemens Smart CCD	Stoe-IPDS-II
θ-range [deg]	1.58–25.03	3.49–25.36	1.64–30.92	1.88–25.83
Index ranges	$-40 \le h \le 40$, $-16 \le k \le 16$, $-43 \le l \le 43$	$-18 \le h \le 19$, $-17 \le k \le 15$, $-27 \le l \le 27$	$-25 \le h \le 24$, $-21 \le k \le 21$, $-27 \le l \le 28$	$-10 \le h \le 10$, $-31 \le k \le 31$, $-26 \le l \le 26$
No. of reflections collected	229 234	34 209	85 684	41 549
No. of independent reflections	30265	9551	15667	9209
R(int.)	0.3309	0.1348	0.0467	0.0656
Absorption correction	empirical	empirical	empirical	semi-empirical from equivalents
Min./max. transmission	0.934/0.9493	0.9171/0.9776	0.833/1.000	0.8781/0.9480
Data/restraints/parameters	30265/414/1513	9551/0/460	15667/0/428	9209/0/424
Goodness of fit on F^2	1.027	0.797	1.051	0.967
Final R indices [$I > 2\sigma(I)$], R1, $wR2$	0.1312, 0.2789	0.0563, 0.0892	0.0444, 0.1154	0.0320, 0.0666
Largest diff. peak/hole [e Å^{-3}]	0.523/–0.386	0.639/–0.590	3.715/–0.642	0.401/–0.191

Thermolysis of (*t*Bu$_3$Si)$_3$P$_5$: A solution of (*t*Bu$_3$Si)$_3$P$_5$ (0.050g, 0.066 mmol) in 1 mL of C$_6$D$_6$ was heated at 120 °C for 24 h. The NMR spectra (^{1}H, ^{13}C, ^{31}P, ^{29}Si) showed only the signals of the bicyclo[1.1.0]tetraphosphane (*t*Bu$_3$Si)$_2$P$_4$ and the deuterated supersilylphosphane *t*Bu$_3$SiPD$_2$. **(*t*Bu$_3$Si)$_2$P$_4$:** ^{1}H NMR (C$_6$D$_6$, internal TMS): δ = 1.21 (br., 6 *t*Bu) ppm. ^{13}C{^{1}H}NMR (C$_6$D$_6$, internal TMS): δ = 26.3 (br., *C*Me$_3$), 31.7 (br., C*Me$_3$*) ppm. ^{29}Si{^{1}H}NMR (C$_6$D$_6$, external TMS): δ = 16.4 (m, 2 Si*t*Bu$_3$) ppm. ^{31}P{^{1}H}NMR (25 °C, C$_6$D$_6$, external H$_3$PO$_4$): δ = –139.1 (t, $^1J_{\mathrm{P,P}}$ = 100.5 Hz; PSi*t*Bu$_3$), –334.4 (t, $^1J_{\mathrm{P,P}}$ = 100.5 Hz) ppm.

***t*Bu$_3$SiPD$_2$:** ^{1}H NMR (C$_6$D$_6$, internal TMS): δ = 1.11 (d, $^4J_{\mathrm{P,H}}$ = 0.46 Hz; 3 *t*Bu) ppm. ^{13}C{^{1}H}NMR (C$_6$D$_6$, internal TMS): δ = 22.8 (d, $^2J_{\mathrm{C,P}}$ = 6.14 Hz, *C*Me$_3$), δ = 30.9 (d, $^3J_{\mathrm{P,C}}$ = 3.0 Hz, C*Me$_3$*) ppm. ^{29}Si{^{1}H}NMR (C$_6$D$_6$, external TMS): δ = 24.0 (d, $^1J_{\mathrm{P,Si}}$ = 30.72 Hz, Si*t*Bu$_3$) ppm. ^{31}P{^{1}H}NMR (25 °C, C$_6$D$_6$, external H$_3$PO$_4$): δ = –268.86 (quint, $^1J_{\mathrm{P,D}}$ = 29.43 Hz) ppm.

Reaction of (*t*Bu$_3$Si)$_3$P$_5$ with CF$_3$CO$_2$H: One drop of CF$_3$CO$_2$H was added to a solution of (*t*Bu$_3$Si)$_3$P$_5$ (0.026 g, 0.0340 mmol) in 1 mL of C$_6$D$_6$. The NMR spectra (^{1}H, ^{13}C, ^{31}P, ^{29}Si, ^{19}F) showed the signals of supersilylphosphenium trifluoroacetate [*t*Bu$_3$SiPH$_3$][CF$_3$CO$_2$], *t*Bu$_3$SiO$_2$CCF$_3$, and P$_4$ as the main products.

[*t*Bu$_3$SiPH$_3$][CF$_3$CO$_2$]: ^{1}H NMR (C$_6$D$_6$, internal TMS): δ = 0.97 (br., 3 *t*Bu) ppm. ^{13}C{^{1}H}NMR (C$_6$D$_6$, internal TMS): δ = 22.3 (br., *C*Me$_3$), 30.8 (br., C*Me$_3$*), 115.4 (q, $^1J_{\mathrm{C,F}}$ = 284.6 Hz, *C*F$_3$), 159.3 (q, $^2J_{\mathrm{C,F}}$ = 84.9 Hz, *C*O$_2$) ppm. ^{29}Si{^{1}H}NMR (C$_6$D$_6$, external TMS): δ = 18.3 (d, $^1J_{\mathrm{P,Si}}$ = 24.3 Hz, Si*t*Bu$_3$).

***t*Bu$_3$SiO$_2$CCF$_3$:** ^{1}H NMR (C$_6$D$_6$, internal TMS): δ = 1.02 (s, 3 *t*Bu) ppm. ^{13}C{^{1}H}NMR (C$_6$D$_6$, internal TMS): δ = 23.2 (s, *C*Me$_3$), 29.2 (s, C*Me$_3$*), 114.8 (q, $^1J_{\mathrm{C,F}}$ = 285.1 Hz, *C*F$_3$) 159.6 (q, $^2J_{\mathrm{CF}}$ = 86.1 Hz, *C*O$_2$) ppm. ^{29}Si{^{1}H}NMR (C$_6$D$_6$, external TMS): δ = 22.8 (s, Si*t*Bu$_3$) ppm.

Photolysis of [(*t*Bu$_3$Si)$_3$P$_5$Ag$_2$]$_2$: A mixture of crystals of [(*t*Bu$_3$Si)$_3$P$_5$Ag$_2$]$_2$·2(C$_6$H$_8$) (0.044 g, 0.021 mmol) and 1 mL of C$_6$D$_6$ was irradiated at ambient temperature for 24 h. After irradiation the NMR spectra (^{1}H, ^{13}C, ^{31}P, ^{29}Si) of the reaction solution showed only the signals of the bicyclo[1.1.0]tetraphosphane (*t*Bu$_3$Si)$_2$P$_4$ and the supersilylphosphane *t*Bu$_3$SiPH$_2$.

(*t*Bu$_3$Si)$_2$P$_4$: ^{1}H NMR (C$_6$D$_6$, internal TMS): δ = 1.21 (br., 6 *t*Bu) ppm. ^{13}C{^{1}H}NMR (C$_6$D$_6$, internal TMS): δ = 26.3 (br., *C*Me$_3$), 31.7 (br., C*Me$_3$*) ppm. ^{29}Si{^{1}H}NMR (C$_6$D$_6$, external TMS): δ = 16.4 (m, 2 Si*t*Bu$_3$) ppm. ^{31}P{^{1}H}NMR (25 °C, C$_6$D$_6$, external H$_3$PO$_4$): δ = –139.1 (t, $^1J_{\mathrm{P,P}}$ = 100.5 Hz, PSi*t*Bu$_3$), –334.4 (t, $^1J_{\mathrm{P,P}}$ = 100.5 Hz) ppm.

***t*Bu$_3$SiPH$_2$:** ^{1}H NMR (C$_6$D$_6$, internal TMS): δ = 1.09 (d, $^4J_{\mathrm{P,H}}$ = 0.49 Hz, 3 *t*Bu) ppm. ^{13}C{^{1}H}NMR (C$_6$D$_6$, internal TMS): δ = 23.1 (d, $^2J_{\mathrm{C,P}}$ = 5.86 Hz, *C*Me$_3$), 30.7 (d, $^3J_{\mathrm{P,C}}$ = 2.44 Hz, C*Me$_3$*) ppm. ^{29}Si{^{1}H}NMR (C$_6$D$_6$, external TMS): δ = 24.1 (d, $^1J_{\mathrm{P,P}}$ = 33.21 Hz, Si*t*Bu$_3$) ppm. ^{31}P{^{1}H}NMR (25 °C, C$_6$D$_6$, external H$_3$PO$_4$): δ = –263.82 (t, $^1J_{\mathrm{P,H}}$ = 185.43 Hz) ppm.

X-ray Crystallographic Study: Data were collected on a Stoe-IPDS-II diffractometer or Siemens CCD three-circle diffractometer. An empirical absorption correction was performed using MULABS[21] and SADABS.[22] Structure solution was performed by direct methods,[23] and structure refinement by full-matrix least-squares on F^2 with SHELXL-97.[24] Hydrogen atoms were placed at ideal positions and refined with fixed isotropic displacement parameters using a riding model. Further details are given in Table 1.

CCDC-249924 (for **2Na**), -249925 (for **[5aNa$_2$(THF)]$_2$**), -253618 (for **[5aAg]$_2$**) and -249926 [for **6(Si*t*Bu$_3$)**] contain the supplementary crystallographic data for this paper. These data can be obtained free of charge from The Cambridge Crystallographic Data Center via www.ccdc.cam.ac.uk/data_request/cif.

Acknowledgments

We are grateful to the University of Frankfurt for funding and the Chemetall GmbH for a gift of *tert*-butyllithium. G. M. wishes to thank the "Fonds der Chemischen Industrie" (FCI) and the "Bundesministerium für Bildung und Forschung" (BMBF) for a Ph. D. grant.

---

[1] N. Wiberg, A. Wörner, K. Karaghiosoff, D. Fenske, *Chem. Ber./Recueil* **1997**, *130*, 135.
[2] N. Wiberg, A. Wörner, H.-W. Lerner, K. Karaghiosoff, D. Fenske, G. Baum, A. Dransfeld, P. von Ragué Schleyer, *Eur. J. Inorg. Chem.* **1998**, 833.
[3] N. Wiberg, *Coord. Chem. Rev.* **1997**, *163*, 217.
[4] H.-W. Lerner, M. Bolte, K. Karaghiosoff, M. Wagner, *Organometallics* **2004**, *23*, 6073.
[5] H.-W. Lerner, M. Wagner, M. Bolte, *Chem. Commun.* **2003**, 990.
[6] N. Wiberg, A. Wörner, H.-W. Lerner, K. Karaghiosoff, H. Nöth, *Z. Naturforsch., Teil B* **1998**, *53*, 1004.
[7] M. Baudler, K. Glinka, *Chem. Rev.* **1993**, *93*, 1623.
[8] H.-G. von Schnering, W. Hönle, *Chem. Rev.* **1988**, *88*, 243.
[9] M. Baudler, *Angew. Chem. Int. Ed. Engl.* **1987**, *26*, 419.
[10] M. Baudler, D. Düster, D. Ouzounis, *Z. Anorg. Allg. Chem.* **1987**, *544*, 87.
[11] M. Detzel, T. Mohr, O. J. Scherer, G. Wolmershäuser, *Angew. Chem. Int. Ed. Engl.* **1994**, *33*, 1110.
[12] E. Urnezius, W. W. Brennessel, C. J. Cramer, J. E. Ellis, P. von Ragué Schleyer, *Science* **2002**, *295*, 832.
[13] I. Krossing, I. Raabe, *Angew. Chem. Int. Ed.* **2001**, *40*, 4406.
[14] M. Gonsior, I. Krossing, L. Müller, I. Raabe, M. Jansen, L. van Wullen, *Chem. Eur. J.* **2002**, *8*, 4475.
[15] S. Böcker, M. Häser, *Z. Anorg. Allg. Chem.* **1995**, *621*, 258.
[16] N. Wiberg, K. Amelunxen, H.-W. Lerner, H. Schuster, H. Nöth, I. Krossing, M. Schmidt-Amelunxen, T. Seifert, *J. Organomet. Chem.* **1997**, *542*, 1.
[17] G. Margraf, I. Sänger, J. W. Bats, M. Wagner, H.-W. Lerner, unpublished results.
[18] M. Baudler, M. Michels, J. Hahn, M. Pieroth, *Angew. Chem. Int. Ed. Engl.* **1985**, *24*, 504.
[19] J. J. Daly, J. Maier, *Nature* **1965**, 208.
[20] R. C. Smith, E. Urnezius, K.-C. Lam, A. Rheingold, J. D. Protasiewicz, *Inorg. Chem.* **2002**, *41*, 5296.
[21] R. H. Blessing, *Acta Crystallogr., Sect. A* **1995**, *51*, 33.
[22] G. M. Sheldrick, SADABS, University of Göttingen, Germany, **2000**.
[23] G. M. Sheldrick, *Acta Crystallogr., Sect. A* **1990**, *46*, 467.
[24] G. M. Sheldrick, *SHELXL-97, A Program for the Refinement of Crystal Structures*, University of Göttingen, Germany, **1997**.

Received: November 22, 2004